

A Kinetic Study of the Folding of Staphylococcal Nuclease Using Size-Exclusion Chromatography†

William Shalongo, M. V. Jagannadham, Paul Heid, and Earle Stellwagen*

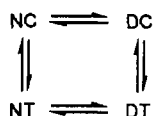
Department of Biochemistry, University of Iowa, Iowa City, Iowa 52242

Received June 5, 1992; Revised Manuscript Received August 27, 1992

ABSTRACT: The kinetics of the hydrodynamic volume change accompanying the reversible unfolding of staphylococcal nuclease have been observed by size-exclusion chromatography at 4 °C and pH 7.0 using the denaturant guanidine hydrochloride. The observed chromatographic profiles have been simulated by a six-component unfolding/refolding mechanism using a consistent set of equilibrium and kinetic parameters. The native protein is an equilibrium mixture of the cis and trans isomers of the peptide bond preceding proline-117. The native conformation containing the cis isomer dominates the equilibrium mixture, is more stable, and unfolds more slowly at its transition midpoint. The denatured protein is an equilibrium mixture of at least four components, the cis/trans isomers of proline-117 and one of the five remaining prolines. The dominant refolding pathway is initiated from the denatured component containing the trans isomer of proline-117. The six-component mechanism is consistent with tryptophan fluorescence kinetic measurements of the wild-type protein and with chromatographic measurements of a mutant P117G protein.

Size-exclusion chromatographic (SEC) measurements can be used to observe the sizable changes in hydrodynamic volume accompanying the reversible unfolding of globular proteins in denaturants. Recent advances in SEC measurements and their analysis (Shalongo et al., 1987, 1989) facilitate measurement of the kinetics of these changes in hydrodynamic volume. In this report, we describe the equilibrium and kinetic parameters associated with the changes in hydrodynamic volume accompanying the reversible unfolding of staphylococcal nuclease. We find these parameters to both complement and extend measurements of the reversible unfolding observed by tryptophan fluorescence, by circular dichroism, and by proton nuclear magnetic resonance (NMR) measurements.

The reversible unfolding of staphylococcal nuclease observed by NMR measurements at the midpoint of its thermal transition, 49 °C (Evans et al., 1989; Alexandrescu et al., 1989, 1990), is described by the four-component mechanism:



In this mechanism, N denotes the native protein, D denotes the denatured protein, C denotes the cis isomer of the peptide bond preceding proline-117 (Cotton et al., 1979; Loll & Lattman, 1989), and T denotes the trans isomer of this peptide bond. The mechanism contains two conformational transitions, NC/DC and NT/DT, which are coupled by two proline peptide isomerization reactions, NC/NT and DC/DT. In contrast, to most proteins, both NC and NT are significantly populated in solutions of the native protein. Recent circular dichroic measurements (Sugawara et al., 1991) indicate that this pertains at 4 °C as well. Component NC is the predominant isomer in solutions of the native protein and is more stable to thermal denaturation. By contrast, component

DT is the predominant isomer in solutions of the denatured protein.

EXPERIMENTAL PROCEDURES

Materials. Staphylococcal nuclease (EC 3.1.4.4) was purified from *Escherichia coli* containing the wild-type staphylococcal nuclease gene (nuc) in the expression plasmid pF0740G405. This organism was kindly supplied by Dr. David Shortle. The enzyme was purified as described by Shortle (1986) and appeared monodisperse when examined by SDS-PAGE and by SEC. Samples of a mutant staphylococcal nuclease where proline-117 is replaced by a glycine (P117G) were also supplied by Dr. David Shortle and used without further purification. The nuclease concentration was determined spectrophotometrically assuming that a 1% solution has an absorbance of 9.3 at 280 nm for an optical cell with a 10-mm light path (Fuchs et al., 1967). Extrapure guanidine hydrochloride (GuHCl) was purchased from Heico. Aqueous solution concentrations of this denaturant were determined using an Abbe Mark II digital refractometer. Toyo Soda 2000SW gel filtration columns, 7.5 × 300 mm, were purchased from Bio-Rad.

Methods. All equilibrium and kinetic measurements were made in solvents containing 25 mM phosphate buffer, 100 mM NaCl, and the indicated concentrations of the denaturant guanidine hydrochloride which were maintained at pH 7.0 and 4 °C. Fluorescence measurements were made using an SLM Model 4800 fluorometer, 295-nm excitation, and a 10-mm square optical cell. Fluorescence equilibrium spectra were analyzed using a two-state mechanism, N/D, as described by Shortle (1986). Fluorescence kinetic profiles were fit either to simultaneous first-order reactions (Kelly & Stellwagen, 1984) or to an explicit reaction mechanism. Chromatographic measurements were made using an IBM LC9533 chromatograph operated by an IBM Model 9000 computer. Elution profiles were obtained using an absorbance flow detector at 225 nm and a solvent flow rate of 1 mL/min. All elution profiles observed in 0.78 M denaturant at pH 7.0 were superimposable with those observed at pH 5.3. Accordingly, it is unlikely that the difference in pH at which the SEC and

† This investigation was supported by U.S. Public Health Service Research Grant GM22109 from the Institute of General Medical Sciences and in part by Institutional Research Fellowship HL07121 from the National Heart, Lung and Blood Institute and by Instrumentation Grant PCM-8313046 from the National Science Foundation.

NMR measurements were performed is consequential to the parameters obtained.

The fraction of denatured protein in a chromatographic elution profile was obtained by partitioning the total peak area into the areas corresponding to the native and denatured protein. A line perpendicular to the base line was dropped either from the minimum between well-resolved peaks or from the point between a peak and a shoulder which corresponds to a maximum in the absolute value of the second derivative. The variation in the fraction of denatured protein obtained from area analysis of duplicate chromatographic profiles is $\pm 2\%$.

Chromatographic Simulations. Each conformational transition, N/D, is characterized by a transition midpoint, a transition width, and a conformational exchange time. The transition midpoint, $[G]_m$, is the denaturant concentration in which both conformations are equally populated. The transition width, $[G]_w$, is the denaturant concentration range which spans the central 80% of the conformational transition. The conformational exchange time is the reciprocal sum of the folding and unfolding rate constants, k_F and k_U . The relationship between the kinetic and equilibrium parameters for a conformational transition in a denaturant concentration, $[G]$, is given by eq 1. Each proline peptide isomerization is

$$\log(k_U/k_F) = \log K = \log([D]/[N]) = 2([G] - [G]_m)/[G]_w \quad (1)$$

characterized by the percentage of protein in the trans isomer at equilibrium and by an isomerization exchange time. The isomerization exchange time is the reciprocal sum of the cis and trans rate constants, k_C and k_T . Among all the parameters which describe a conformational transition and a proline peptide isomerization, only the conformational exchange time is dependent on denaturant concentration.

The SEC of a protein undergoing a transition can be described by three events. The first chromatographic event is sieving, the transfer of protein between chromatographic regions, r , during discrete time intervals, i , which is described by eq 2–4 using the native protein as an example. In these

$$m_N = t_x/t_N \quad (2)$$

$$[N]_{r,i}^t = (1 - m_N)[N]_{r,i-1}^e + m_N[N]_{r-1,i-1}^e \quad (3)$$

$$[N]_{1,i}^t = (1 - m_N)[N]_{1,i-1}^e + m_N f_N c_w \quad (4)$$

equations, m_N is the partition coefficient for the native protein, t_x is the elution time for a totally excluded molecule, t_N is the elution time for the native protein, f_N is the fraction of native protein in the injected sample, and c_w is either c_i/w if $w \geq i$ or 0 if $w < i$, where w is the time required to transfer all of the total injected protein sample, c_i , into the column. Superscripts t and e denote the concentration of native protein after the transfer event in the current time interval and after all events at the end of the previous time interval, respectively.

The second event is apparent matrix binding which models the asymmetry of native and denatured protein peaks in terms of an apparent, weak, reversible binding to the chromatographic matrix. Apparent matrix binding is described by eq 5 and 6 using the native protein as an example. In these

$$[N]_{r,i}^u = [N]_{r,i}^t - [N]_{r,i}^t(1 - e^{-k_{aN}\Delta t}) + [N]_{r,i}^b(1 - e^{-k_{dN}\Delta t}) \quad (5)$$

$$[N]_{r,i}^b = [N]_{r,i}^b + [N]_{r,i}^t(1 - e^{-k_{aN}\Delta t}) - [N]_{r,i}^b(1 - e^{-k_{dN}\Delta t}) \quad (6)$$

equations, k_{aN} and k_{dN} are the apparent association rate constant and the apparent dissociation rate constant for apparent matrix binding, respectively, and Δt is the duration of the time interval. The superscripts u and b denote the unbound protein and the bound protein, respectively, at the end of the apparent matrix binding event. While eq 2–6 are written for the native protein, N , the reader should understand that analogous equations must be written for the denatured protein, D , as well.

The third event is the equilibration of the protein between the native and denatured protein components in each chromatographic region during the current time interval. This equilibration proceeds through an explicit mechanism of coupled conformational transitions and proline peptide isomerization reactions. A conformational transition is described by eq 7 and 8 in which $[N]_{r,i}^e$ and $[D]_{r,i}^e$ are the concentrations

$$[N]_{r,i}^e = [N]_{r,i}^u - [N]_{r,i}^u(1 - e^{-k_{UN}\Delta t}) + [D]_{r,i}^u(1 - e^{-k_{FN}\Delta t}) \quad (7)$$

$$[D]_{r,i}^e = [D]_{r,i}^u + [N]_{r,i}^u(1 - e^{-k_{UN}\Delta t}) - [D]_{r,i}^u(1 - e^{-k_{FN}\Delta t}) \quad (8)$$

of the native and denatured protein, respectively, after the conformational equilibration has proceeded for the time interval Δt . A proline peptide isomerization reaction between C and T is described by eq 9 and 10 in which $[C]_{r,i}^e$ and $[T]_{r,i}^e$

$$[C]_{r,i}^e = [C]_{r,i}^u - [C]_{r,i}^u(1 - e^{-k_{CT}\Delta t}) + [T]_{r,i}^u(1 - e^{-k_{CT}\Delta t}) \quad (9)$$

$$[T]_{r,i}^e = [T]_{r,i}^u + [C]_{r,i}^u(1 - e^{-k_{CT}\Delta t}) - [T]_{r,i}^u(1 - e^{-k_{CT}\Delta t}) \quad (10)$$

are the concentrations of the cis and trans proline isomers, respectively, after the isomerization equilibration has proceeded for the time interval Δt . Analogous expressions must be written for each conformational transition and proline peptide isomerization reaction in the mechanism. The continuous flow among components within an explicit mechanism can be calculated as a series of transitions between pairs of components during each time interval, assuming the change in concentration of each component is small relative to the total concentration of protein.

Numerical iteration of equations 1–10 results in a simulated chromatographic profile ($[N]_i + [D]_i$) as a function of chromatographic time, $i\Delta t$. These equations have been incorporated into a menu-driven FORTRAN program which coplots the simulated and observed chromatographic profiles. Operation of the program requires specification of parameters describing each of the three events in SEC: sieving, apparent matrix binding, and equilibration of protein among each component in the reaction mechanism. Simulations of the peak in each base-line zone indicate that the sieving column contained 300 ± 50 chromatographic regions. The asymmetry of the peaks in each base-line zone was simulated using apparent association rate constants of 0.019 ± 0.003 and $0.030 \pm 0.000 \text{ min}^{-1}$, and apparent dissociation rate constants of 1.02 ± 0.18 and $6.00 \pm 0.00 \text{ min}^{-1}$, for the native and denatured protein, respectively. Elution time measurements for the peak in each base-line zone indicate that the elution times for the native and denatured proteins differ by $1.60 \pm 0.01 \text{ min}$. The transition width for all conformational transitions was held

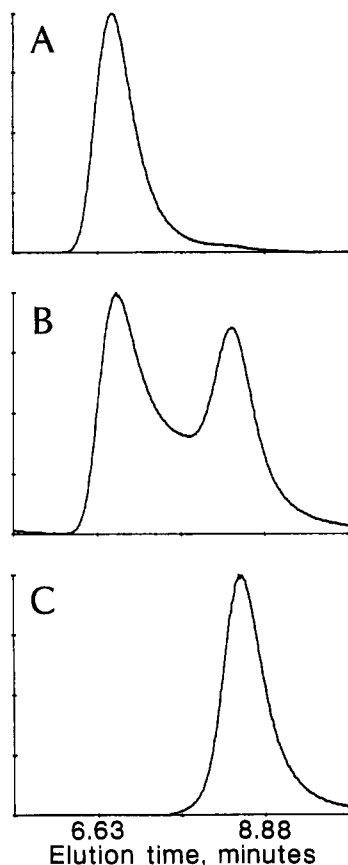


FIGURE 1: Wild-type nuclease equilibrium chromatographic profiles. Solutions containing 6 μ M nuclease, 25 mM phosphate, 100 mM NaCl, and the indicated concentration of denaturant were each maintained at pH 7.0 and 4 $^{\circ}$ C for at least 24 h. A 15- μ L aliquot of each protein solution was then injected into a column equilibrated with the same solvent at 4 $^{\circ}$ C. The denaturant concentration in panel A was 1.01 M, in panel B 0.82 M, and in panel C 0.50 M.

to 0.40 M denaturant, the width of the overall transition observed by equilibrium measurements. Equilibrium and kinetic parameters for each component were then varied until the observed and simulated chromatographic profiles were coincident.

RESULTS AND DISCUSSION

Chromatographic Measurements of Wild-Type Nuclease. Equilibrium chromatographic profiles were obtained by equilibration of a protein sample and a SEC column with the same denaturant concentration prior to injection of the protein into the column. Typical equilibrium profiles for wild-type nuclease are illustrated in Figure 1. A single nearly symmetrical peak is observed in the equilibrium profiles obtained in 1.01 and 0.50 M denaturant (Figure 1A,C, respectively). The large decrease in the elution time of the protein, 1.60 min, accompanying this increase in denaturant concentration indicates a substantive increase in the hydrodynamic volume of nuclease. The decrease in elution time for nuclease, which contains 149 residues, is identical with that accompanying the denaturation of horse myoglobin which contains 153 residues. This comparison suggests that the decrease in elution time observed for nuclease is appropriate for the denaturation of a globular protein containing about 150 residues and no disulfide bonds. Accordingly, the nuclease component having an elution time of about 8.5 min will be assumed to represent the compact native protein, and the component having an elution time of about 6.9 min will be assumed to represent the denatured protein.

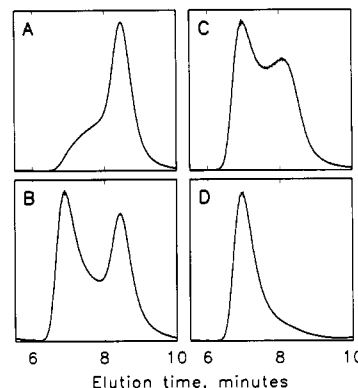


FIGURE 2: Representative unfolding, equilibrium, multimixing, and refolding chromatographic profiles observed using wild-type nuclease. All profiles were obtained using a column equilibrated with 25 mM phosphate, 100 mM NaCl, and 0.82 M denaturant maintained at pH 7.0 and 4 $^{\circ}$ C. The unfolding profile in panel A was observed following injection of the native protein. The equilibrium profile in panel B was observed following injection of protein equilibrated with the chromatographic solvent for 24 h. The multimixing profile observed in panel C was observed following injection of protein exposed to 6.5 M denaturant at pH 7.0 and 4 $^{\circ}$ C for 15 s. The refolding profile in panel D was observed following injection of protein equilibrated with 6.5 M denaturant at pH 7.0 and 4 $^{\circ}$ C for 24 h.

Equilibrium profiles observed in denaturant concentrations between 0.5 and 1.01 M are bimodal. A typical equilibrium profile observed for wild-type nuclease in 0.82 M denaturant is illustrated in Figure 1B. Such an equilibrium profile is characteristic for reversible denaturation in slow exchange which appears to be dominated by a single component in the native protein and a single component in the denatured protein. These components would correspond to NC and DT, respectively, in the four-component NMR mechanism. The near-equivalence of the native and denatured components in the equilibrium profile illustrated in Figure 1B suggests that 0.82 M guanidine hydrochloride is near the midpoint of the equilibrium transition of the protein.

Unfolding profiles were obtained by injection of native nuclease into a column equilibrated with a denaturant concentration greater than 0.5 M. A typical unfolding profile observed in 0.82 M denaturant is illustrated in Figure 2A. The amount of denatured protein evident in this unfolding profile is less than that observed in the equilibrium profile obtained in the same denaturant concentration (Figure 2B). This comparison suggests either that unfolding is slow in 0.82 M denaturant or that the native protein is a mixture of two or more populations with distinct unfolding transitions. Each of the unfolding profiles was resolved into the percentage of denatured protein as described under Methods. The results of these analyses at discrete denaturant concentrations are illustrated by the open circles in Figure 3A. The bimodal character of the relationship in Figure 3A suggests that (i) the unfolding of two different native components is observed, (ii) the two native components do not rapidly interconvert, and (iii) the dominant native component is more stable. These features are consistent with the four-component NMR mechanism in which the dominant, more stable native component is NC.

Injection of native nuclease into excess denaturant would be expected to rapidly denature all the protein, generating a mixture of about 80% DC and 20% DT. Tryptophan fluorescence measurements indicate that nuclease is completely denatured by exposure to 6 M guanidine hydrochloride for 15 s at 4 $^{\circ}$ C. Injection of such a briefly denatured protein into a SEC column containing less than 1.0 M denaturant would facilitate refolding of the protein. These profiles are termed

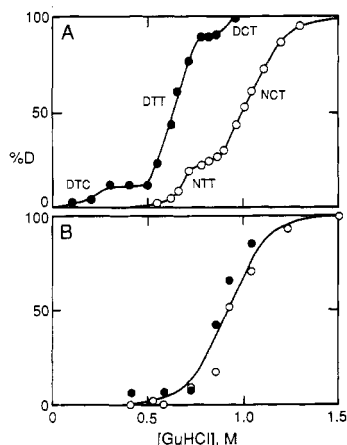


FIGURE 3: Percentage of denatured protein estimated in unfolding and refolding profiles observed in different denaturant concentrations. Each profile was parsed in the fractional area associated with the denatured protein as described under Methods. An estimated variance of $\pm 2\%$ denatured protein was determined by parsing the profiles resulting from multiple injections at the same denaturant concentration. The open circles indicate the average of the estimates of the denatured protein in unfolding profiles, and the filled circles indicate the average of the estimates of the denatured protein in refolding profiles. The three-letter notation indicates the component in the six-component mechanism whose unfolding or refolding predominates in the adjacent region of the estimated transition. The wild-type nuclease is shown in panel A, and the mutant P117G nuclease is shown in panel B. The curves in panel A were drawn to group the unfolding and refolding measurements and do not reflect the fractional area of the denatured protein obtainable from chromatographic simulations. The curve in panel B describes a conformational transition with a midpoint of 0.94 M and a transition width of 0.4 M. The transition midpoint is within the range of midpoints observed from simulations of the mutant P117G nuclease listed in Table I.

multimixing profiles since they originate from a protein sample which is not in equilibrium with its solvent. The multimixing profile observed from a column containing 0.82 M denaturant is illustrated in Figure 2C. This multimixing profile is similar to the equilibrium profile observed in the same denaturant concentration (Figure 2B). Such similarity suggests that the midpoint for the NC/DC conformational transition is above 0.82 M and that the refolding of DC is moderately fast in this denaturant concentration. The well-defined valley separating the native and denatured protein in the multimixing profile further suggests that the injected DC does not persist during chromatography but either refolds to NC or isomerizes to DT with comparable rates.

Refolding profiles were obtained by equilibration of protein in 6 M denaturant at 4 °C for 24 h prior to injection into a SEC column. Such an extended equilibration facilitates equilibration of DC and DT prior to the initiation of refolding by injection into the column. The refolding profile observed in 0.82 M denaturant is illustrated in Figure 2D. In contrast to the multimixing profile obtained in the same solvent (Figure 2C), only a small fraction of the injected denatured protein refolds during chromatography. This suggests that the major denatured component initially present, DC, has isomerized to the other denatured isomer, DT, as predicted by the four-component NMR mechanism and suggests either that the midpoint for the refolding transition for DT is below 0.82 M denaturant or that the refolding kinetics are very slow compared to chromatographic time. The latter suggestion is not supported by the tryptophan fluorescence measurements described below. Further, the thermodynamic balance of the four-component NMR mechanism requires a low midpoint for the NT/DT conformational transition.

Each of the refolding profiles were resolved into the percentage of denatured protein as described under Methods.

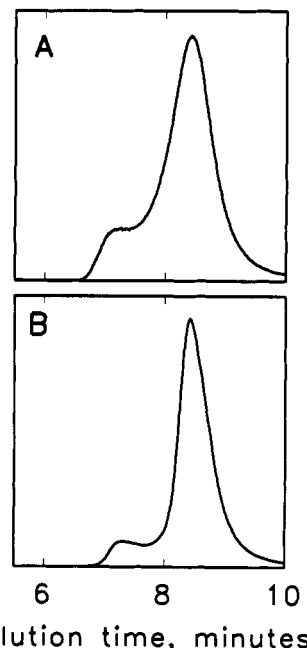
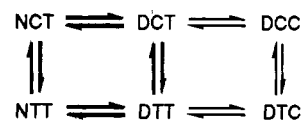


FIGURE 4: Refolding profiles observed in low concentrations of denaturant. Profile A is the refolding profile of the wild-type nuclease in 0.5 M denaturant. Profile B is the refolding profile of the mutant P117G nuclease in 0.58 M denaturant.

The results of these analyses at discrete denaturant concentrations are illustrated by the filled circles in Figure 3A. The trimodal character of this relationship suggests that (i) the refolding of three different denatured components is observed, (ii) the three denatured components do not rapidly interconvert, and (iii) the dominant denatured component has intermediate stability. The observation of three different denatured components requires expansion of the four-component NMR mechanism. The refolding observed during chromatography in denaturant concentrations greater than 0.5 M likely reflects the refolding of the dominant component, DC, and the minor component, DT, in the four-component NMR mechanism. Such assignment requires that the refolding of the remaining denatured component occurs in denaturant concentrations less than 0.5 M. Inspection of the refolding profile observed in 0.5 M denaturant (Figure 4A) clearly indicates the presence of this unfolded component.

An attractive expansion of the four-component NMR mechanism involves a cis/trans isomerization of one of the remaining five proline peptide bonds in nuclease. Since the peptide bond preceding each of these proline residues is trans in the native protein (Cotton et al., 1979; Loll & Lattman, 1989), the nonnative peptide isomer in the denatured protein must be cis. A minimal expansion of the four-component NMR mechanism to accommodate a second proline peptide isomerization is shown below as a six-component mechanism.



The first letter in the designation for each component indicates either a native or a denatured protein, the middle letter indicates the isomer of a peptide bond preceding Pro-117, and the final letter indicates the isomer of the peptide bond preceding a different proline residue. In this presentation of the six-component mechanism, the boldface arrows indicate the four-component mechanism derived from NMR measurements.

Table I: Denaturant-Independent Parameters at 4 °C

reaction/parameter	fluorescence unfolding	SEC unfolding	SEC multimixing	SEC refolding
Wild-Type Nuclease				
NCT/DCT midpoint, M	1.05 ± 0.01	1.10 ± 0.02	1.01 ± 0.03	1.03
NTT/DTT midpoint, M	0.64 ± 0.01	0.62 ± 0.02	0.62	0.62 ± 0.01
NCT/NTT % NCT	80	80 ± 2	87 ± 2	83
exchange time, s	300	300	300	300 ± 25
DCT/DTT and DCC/DTC % DTC or % DCC	7	5	10 ± 1	5
exchange time, s	190	190	190 ± 10	190
DTC/DCC and DTT/DTT % DCC or % DTC	25	25	25	25
exchange time, s	750	750	750	750 ± 50
Mutant P117G Nuclease				
NTT/DTT midpoint, M		0.95 ± 0.03		0.94 ± 0.01
DTT/DTC % DTC		20		20 ± 2
exchange time, s		250		250 ± 50

An alternative expansion of the four-component NMR mechanism suggests that the refolding of 10% of the denatured protein is delayed by transient aggregation upon dilution of the denaturant. This suggestion is less likely for two reasons. First, the fraction of denatured protein whose refolding is delayed is independent of the concentration of denatured protein injected in the column. The same refolding profile was observed in 0.50 M denaturant upon injection of 15 μ L of denatured protein whose concentration ranged from 1 to 10 mg/mL. Second, no aggregated protein is observed in the refolding profiles at any denaturant concentration. Aggregated protein would elute prior to the elution position of monomeric denatured protein, and none is seen.

Chromatographic Simulations of Wild-Type Nuclease. The quantitative analysis of SEC profiles was initiated by simulation of unfolding profiles using two independent conformational transitions. Multimixing profiles were simulated next to determine the parameters for the proline peptide isomerization in the denatured protein. The unfolding and multimixing profiles were then simulated using a four-component mechanism to refine the parameters for each conformational transition and each proline peptide isomerization. Refolding profiles obtained in denaturant concentrations greater than 0.5 M were next simulated using a four-component mechanism to further refine these parameters. Finally, all of the observed chromatographic profiles, unfolding, multimixing, and refolding, were simulated at all denaturant concentrations using the six-component mechanism to complete the parameter refinement. Superimpositions were achieved using the denaturant-independent parameters listed in Table I and the denaturant-dependent conformational exchange times presented in Figure 5.

Assessment of the SEC Simulations. An acceptable unfolding/refolding mechanism must accommodate the principal chromatographic features observed for staphylococcal nuclease, namely, the two conformational transitions observed in unfolding profiles, the proline peptide isomerization observed in multimixing profiles, and the generation of denatured components which only directly refold in denaturant concentrations below 0.5 M.

An acceptable mechanism must also simulate ALL of the observed profiles with a self-consistent set of denaturant-independent and denaturant-dependent parameters. Each of the denaturant-independent parameters requires only a very modest variance in order to simulate all the chromatographic profiles as indicated in Table I. The exchange times for the

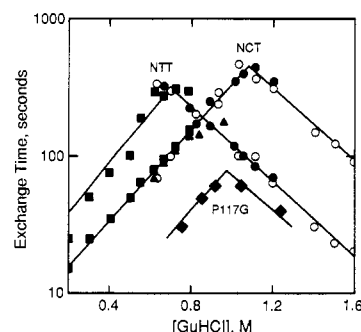


FIGURE 5: Exchange times for the observed conformational transitions. Exchange times denoted by filled circles, filled triangles, and filled squares were obtained by simulation of SEC unfolding, multimixing, and refolding profiles, respectively, for the wild-type nuclease. Exchange times denoted by filled diamonds were obtained by simulation of SEC unfolding and refolding profiles for the mutant P117G nuclease. The exchange times denoted by open circles were obtained by simulation of fluorescence unfolding measurements for the wild-type nuclease. The inverted triangles describing the exchange times for the conformational transitions involving the native components NTT and NCT in the six-component mechanism (NT and NC in the four-component mechanism) are labeled.

proline peptide isomerization reactions fall within the range of protein proline peptide exchange times reported at 4 °C (Ridge et al., 1981; Crisanti & Matthews, 1981; Goto et al., 1979). The denaturant-dependent parameters, namely, the conformational exchange times, are presented in Figure 5. The exchange times for each conformational transition exhibit a triangular semilogarithmic dependence on denaturant concentration. The apex of each triangle is within 0.06 M of the midpoint for each transition. These features are characteristic for the denaturant dependence of conformational transitions.

The loss of the components DCC and DTC from refolding profiles obtained in denaturant concentrations less than 0.3 M indicates that these components can each refold prior to peptide isomerization using conformational refoldings having midpoints less than 0.3 M. Unfortunately, the refolding profiles do not provide sufficient sensitivity to establish these midpoints with precision since no multimixing protocol is accessible to transiently enhance the relative abundance of components DCC and DTC. Within the precision of the SEC measurements, no evidence exists that NCC and NTC are populated in the native protein.

Comparison with NMR Measurements. The parameters for the conformational transitions NCT/DCT and NTT/

DTT obtained from the analysis of NMR measurements and from the analysis of SEC measurements compare favorably. The NMR measurements find NCT to be more stable to thermal denaturation while the SEC measurements find NCT to be more stable to guanidine hydrochloride denaturation. The exchange times for the refolding of DCT and the refolding of DTT obtained from the NMR measurements in the absence of denaturant at 49 °C are within a factor of 2. The exchange times for the refolding of DCT and DTT in the absence of denaturant at 4 °C, obtained by the extrapolation of the values in Figure 5, are also within a factor of 2. The activation energy for the unfolding of NCT and NTT in the absence of denaturant is 12.0 ± 1.5 kcal/mol, a value within the range observed for conformational transitions (Joly, 1965).

The exchange times for the peptide isomerization of Pro-117 obtained from analysis of NMR and SEC measurements also compare favorably. The exchange times for the peptide isomerization obtained from analysis of NMR measurements at 49 °C and from analysis of SEC measurements at 4 °C can be related by an activation energy using the Arrhenius equation. The isomerization in the native protein has an activation energy of 23.5 kcal/mol and in the denatured protein an activation energy of 24.3 kcal/mol. These activation energies are typical for proline peptide isomerizations in proteins (Goto et al., 1979; Ridge et al., 1981; Rehage & Schmid, 1982). The fractional concentrations of components arising from the isomerization of Pro-117 in the denatured protein also compare favorably. The NMR analysis at 49 °C finds 96% of this bond in the trans isomer with a range of 73–98%, while the SEC analysis at 4 °C finds 93% with a range of 90–95%. However, an apparent contradiction between the NMR analysis and the SEC analysis appears when the fractional concentrations of components arising from the isomerization of Pro-117 in the native protein are compared. The NMR analysis at 49 °C finds 83% of this bond in the cis isomer with a range of 67–96%; the SEC analysis at 4 °C finds 82% with a range of 80–87%. The NT/NC reaction has an enthalpy of -45 kJ/mol (Evans et al., 1989), which would predict an equilibrium concentration of NT at 4 °C of about 1%. However, a linear extrapolation of the NC/NT equilibrium constant from 49 to 4 °C is suspect because the temperature dependence of the enthalpy and entropy of unfolding (Privalov & Gill, 1988; Privalov, 1989) predicts the possibility of low-temperature instability for the native protein (Dill et al., 1989). Calculation of the thermal dependence of the free energy from equilibrium fluorescence measurements indicates that the protein is maximally stable at 15 °C and is less stable at colder temperatures (Nakano & Fink, 1990). Therefore, an appreciable population of the less stable NT can exist in the native nuclease as indicated by the SEC analysis. This is confirmed by CD measurements of denaturant-induced unfolding at 4.5 °C (Sugawara et al., 1991), where both isomeric components of native nuclease persist at the low temperatures in which our SEC and fluorescence measurements were made.

Comparison with Fluorescence Measurements. The substantial change in the fluorescence emission of tryptophan-140 has been used to observe the reversible denaturation of nuclease (Shortle, 1986). Accordingly, tryptophan fluorescence measurements were performed under the same conditions used for the SEC measurements to spot-check the results of the chromatographic analysis. These spot-checks indicated that the fluorescence measurements are consistent with the six-component mechanism. The first check was to determine the ability of the SEC measurements and the fluorescence measurements to describe the overall transition at equilibrium.

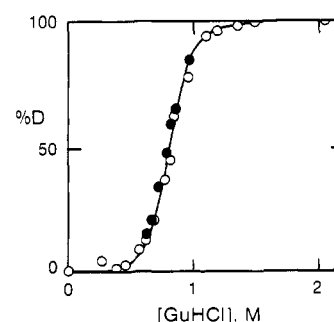


FIGURE 6: Equilibrium transitions for the wild-type nuclease. All measurements were obtained at 4 °C in 10 mM NaCl and 25 mM phosphate buffer, pH 7.0. The open circles indicate fluorescence measurements, and the filled circles indicate SEC measurements.

The fluorescence measurements were analyzed assuming the traditional two-component mechanism, N/D. The results of such analysis are indicated by the open circles in Figure 6. The SEC equilibrium profiles were simulated assuming the same two-component mechanism and a transition midpoint of 0.79 ± 0.01 M. These simulations resolve each profile into the fractional population of N and D. The results of the two-component SEC analyses are indicated by the filled circles in Figure 6. It should be noted that the fluorescence measurements and the SEC measurements describe a common transition. This concurrence does NOT demonstrate that the reversible unfolding of nuclease is truly a two-component mechanism. Rather, the concurrence demonstrates that if a two-component mechanism is assumed for both analyses, then the fluorescence measurements and the SEC measurements observe the same denaturant-dependent transition.

A second check was the ability of each measurement to observe the same kinetic event. The most accessible kinetic event in either the four-component mechanism or the six-component mechanism is the unfolding of the native protein. Most of the fluorescence unfolding time courses could only be fit using two exponentials, indicating the observation of at least two reactions. However, the fractional amplitude and exchange times associated with each exponential did not generate a systematic dependence on denaturant concentration. This suggests that the two reactions are not parallel and independent but are coupled in a manner suggested by the four-component NMR mechanism. Accordingly, it was found that the fluorescence unfolding time courses could be simulated using either the four-component mechanism or the six-component mechanism, the denaturant-independent parameters listed in Table I, and the denaturant-dependent exchange times illustrated by the open circles in Figure 5. It should be remembered that the four-component mechanism is contained within the six-component mechanism. The correspondence of the parameters obtained by the simulation of SEC unfolding profiles and fluorescence unfolding time courses suggests that both measurements are observing the same kinetic events.

A third check involved the role of proline peptide isomerization. Fluorescence refolding time courses are resolvable into three kinetic phases, termed the fast kinetic phase, the middle kinetic phase, and the slow kinetic phase, respectively. Fluorescence multimixing measurements indicate that the middle kinetic phase and the slow kinetic phase are generated in the denatured state at the expense of the fast kinetic phase. This corresponds to the dispersal of DCT among DCC, DTT, and DTC during denaturation. The slow kinetic phase is denaturant-independent and has a time constant of 950 ± 90 s. The time constant observed by fluorescence for a conformational transition preceded by an obligatory slower proline peptide isomerization reaction will represent the unidirectional

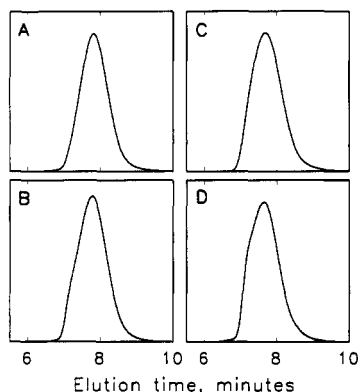


FIGURE 7: Representative unfolding, equilibrium, multimixing, and refolding chromatographic profiles observed using mutant P117G nuclease. All profiles were obtained using a column equilibrated with 25 mM phosphate, 100 mM NaCl, and 0.92 M denaturant maintained at pH 7.0 and 4 °C. The unfolding profile in panel A was observed following injection of the native protein. The equilibrium profile in panel B was observed following injection of protein equilibrated with the chromatographic solvent for 24 h. The multimixing profile observed in panel C was observed following injection of protein exposed to 6.5 M denaturant at pH 7.0 and 4 °C for 15 s. The refolding profile in panel D was observed following injection of protein equilibrated with 6.5 M denaturant at pH 7.0 and 4 °C for 24 h.

proline peptide isomerization reaction rate in the direction of folding. In this case, the observed time constant of 950 ± 90 s would represent the unidirectional rate constant for the DCC/DCT and DTC/DTT proline peptide isomerization reactions. The bidirectional exchange time and equilibrium constant for the DCC/DCT and DTC/DTT proline peptide isomerization reactions obtained from the analysis of SEC measurements would predict a unidirectional rate constant of 1000 s, a value within the range of the observed fluorescence slow kinetic phase time constant.

Comparison with SEC Measurements of Mutant P117G Nuclease. Replacement of proline-117 in wild-type nuclease by a glycine residue should eliminate all the components in the upper line of the six-component mechanism, namely, components NCT, DCT, and DCC. Accordingly, the unfolding kinetics of this mutant protein should be monophasic and the its refolding kinetics should be biphasic if the six-component mechanism for the wild-type protein is appropriate.

Representative unfolding, equilibrium, multimixing, and refolding chromatographic profiles observed for the P117G mutant nuclease are illustrated in Figure 7. Comparable chromatographic profiles observed for the wild-type nuclease are illustrated in Figure 2. These comparisons indicate that the conformational transitions of the mutant nuclease involve fewer components which display faster kinetics. The unfolding chromatographic profiles of the mutant nuclease appear monophasic as shown in Figure 3B. The refolding chromatographic profiles appear biphasic with about 10% of the denatured protein refolding in a slower kinetic phase as shown by the profile in Figure 4B and the filled circles in Figure 3B.

The quantitative simulation of the mutant P117G nuclease SEC profiles was initiated using a three-component mechanism, $\text{NTT} \rightleftharpoons \text{DTT} \rightleftharpoons \text{DTC}$, which is the lower line of the six-component mechanism. Simulations were initiated using a midpoint for the conformational transition, NTT/DTT , of 0.9 M (Figure 3B), an exchange time for the proline peptide isomerization, DTT/DTC , of 750 s, and 75% of the denatured protein in the trans isomer. Each of these values and also the exchange times for the conformational transition were refined by simulation.

All of the chromatographic profiles obtained for the mutant protein can be simulated using the three-component mech-

anism, the denaturant-independent parameters shown in Table I, and the denaturant-dependent conformational exchange times shown in Figure 5. Again, the coincidence of all the observed and simulated chromatographic profiles requires only a modest variation in the denaturant-independent parameters as shown in Table I. The conformational exchange times generate a triangular semilogarithmic dependence on denaturant concentration with the apex at the midpoint of the conformational transition.

Most significantly, the proline peptide isomerization evident in the denatured wild-type protein which does not involve proline-117 is retained in the P117G mutant protein. Replacement of proline-117 with glycine increases the stability of the component NTT to denaturation as shown in Table I. This parallels the increased thermostability of the mutant protein observed by NMR measurements (Evans et al., 1987). The relationship of the triangular semilogarithmic relationships shown in Figure 5 suggests that the mutant P117G nuclease may be an equilibrium mutant (Beasty et al., 1986) of the NTT component of the wild-type protein.

REFERENCES

- Alexandrescu, A. T., Ulrich, E. L., & Markley, J. L. (1989) *Biochemistry* 28, 204–211.
- Alexandrescu, A. T., Hinck, A. P., & Markley, J. L. (1990) *Biochemistry* 29, 4516–4525.
- Beasty, A. M., Hurle, M. R., Manz, J. T., Stackhouse, T., Onuffer, J. J., & Matthews, C. R. (1986) *Biochemistry* 25, 2965–2974.
- Brandts, J. F., Halverson, H. R., & Brennan, M. (1975) *Biochemistry* 14, 4953–4963.
- Cotton, F. A., Hazen, E. E., Jr., & Legg, M. J. (1979) *Proc. Natl. Acad. Sci. U.S.A.* 76, 2551–2555.
- Crisanti, M. M., & Matthews, C. R. (1981) *Biochemistry* 20, 2700–2706.
- Dill, K. A., Alonso, D. O. V., & Hutchinson, K. (1989) *Biochemistry* 28, 5439–5449.
- Evans, P. A., Dobson, C. M., Kautz, R. A., Hatfull, G., & Fox, R. O. (1987) *Nature (London)* 329, 266–268.
- Evans, P. A., Kautz, R. A., Fox, R. O., & Dobson, C. M. (1989) *Biochemistry* 28, 362–370.
- Fuchs, S., Cuatrecasas, P., & Anfinsen, C. B. (1967) *J. Biol. Chem.* 242, 4768–4770.
- Goto, Y., Azuma, T., & Hamaguchi, K. (1979) *J. Biochem.* 85, 1427–1438.
- Joly, M. (1965) *Denaturation of Proteins*, pp 209–214, Academic Press, New York.
- Kelley, R. F., & Stellwagen, E. (1984) *Biochemistry* 23, 5095–5102.
- Loll, P. J., & Lattman, E. E. (1989) *Proteins: Struct., Funct., Genet.* 5, 183–201.
- Nakano, T., & Fink, L. A. (1990) *J. Biol. Chem.* 265, 12356–12362.
- Privalov, P. L. (1989) *Annu. Rev. Biophys. Biophys. Chem.* 18, 47–69.
- Privalov, P. L., & Gill, S. J. (1988) *Adv. Protein Chem.* 39, 191–234.
- Rehage, A., & Schnid, F. X. (1982) *Biochemistry* 21, 1499–1505.
- Ridge, J. A., Baldwin, R. L., & Labhardt, A. L. (1981) *Biochemistry* 20, 1622–1630.
- Shalongo, W., Ledger, R., Jagannadham, M. V., & Stellwagen, E. (1987) *Biochemistry* 26, 3135–3142.
- Shalongo, W., Jagannadham, M. V., Flynn, C., & Stellwagen, E. (1989) *Biochemistry* 28, 4820–4825.
- Shortle, D. (1986) *J. Cell. Biochem.* 30, 281–289.
- Sugawara, T., Kuwajima, K., & Sugai, S. (1991) *Biochemistry* 30, 2698–2706.